SCIENTIA NATURALIS
Scientia Naturalis, v. 7, n. 1, p. 100-125, 2025
Home page: http://revistas.ufac.br/revista/index.php/SciNat
DOI: https://doi.org/10.29327/269504.7.1-9
ISSN 2596-1640

Performance of a downdraft fixed bed gasifier employing air as the gasifying agent and eucalyptus chips in two reactor configurations

Diogo Santos Silva[1*], Luiz Eduardo Pizarro Borges[2], Fábio Bellot Noronha[3]

[1]Discente do Instituto Militar de Engenharia, Praça General Tibúrcio, Praia Vermelha, Rio de Janeiro-RJ, Brasil. [2]Docente do Instituto Militar de Engenharia, Praça General Tibúrcio, Praia Vermelha, Rio de Janeiro-RJ, Brasil. [3]Pesquisador do Instituto Nacional de Tecnologia, Avenida Venezuela, 82, Centro, Rio de Janeiro-RJ, Brasil. *diogofritz@yahoo.com.br

Recebido em: 10/06/2024 **Aceito em: 17/01/2025** **Publicado em: 10/05/2025**

DOI: https://doi.org/10.29327/269504.7.1-9

ABSTRACT

The study of gasification applied to biomass waste has emphasis due to the potential for producing energy with low environmental impact and obtaining chemical products (H_2, CO, CO_2, N_2, light hydrocarbons such as CH_4, C_2H_4, C_2H_6 and others). Efforts were concentrated on the study and optimization of a pilot downdraft gasification unit, with air as the gasifying agent and eucalyptus chips as the fuel in two configurations. The limitations of altering the temperature gradient inside the reactor and the benefit of volumetric expansion inside the reactor for the gas were observed. From 0.6 kg of chips in the optimized condition, 1.25 m^3/h of synthesis gas volume was produced, with a biomass consumption rate (BCR) of 2.4 kg/h, a gas production rate (GPR) of 0,76 Nm^3/ Kg, and an average production of 0.8 g/Nm^3 per run. The performance of the gasifier produced at an equivalence ratio (Φ) of 0.28 a lower heating value (LHV) of the gas of 3.19 MJ/Nm^3, carbon conversion efficiency (CCE) of 68.09% and cold gas efficiency (ECG) of 14.68% to obtain 11% H_2, 59.26% N_2, 11.64% CO, 1.50% CH_4 and 16.60% CO_2.

Keywords: Downdraft. Eucalyptus. Tar.

Performance da planta piloto de leito fixo downdraft empregando o agente gaseificante ar na gaseificação do cavaco de eucalipto em duas configurações de reator

RESUMO

O estudo da gaseificação aplicada a resíduos de biomassa ganhou destaque pelo potencial de produção de energia com baixo impacto ambiental e obtenção de produtos químicos (H_2, CO, CO_2, N_2, hidrocarbonetos leves como CH_4, C_2H_4, C_2H_6 e outros). Concentrou-se esforços no estudo e otimização de uma unidade piloto de gaseificação downdraft, com ar como agente gaseificador e cavaco de eucalipto como combustível em duas configurações. Foram observadas as limitações da alteração do gradiente de temperatura no interior do reator e o benefício da expansão volumétrica no interior do reator para o gás. A partir de 0,6 kg de cavacos de eucalipto, foram produzidos 1,25 m^3/h de volume de gás de síntese, com uma taxa de consumo de biomassa (BCR) de 2,4 kg/h, uma taxa de produção de gás (GPR) de 0,76 Nm^3/Kg e uma produção média de 0,8 g/Nm^3 por corrida. O desempenho do gaseificador produziu a uma razão de equivalência (Φ) de 0,28 um valor de aquecimento inferior (LHV) do gás de 3,19 MJ/Nm^3, eficiência de conversão de carbono (CCE) de 68,09% e eficiência de gás frio (ECG) de 14,68% para obter 11% H_2, 59,26% N_2, 11,64% CO, 1,50% CH_4 e 16,60% CO_2.

Palavras-chave: Downdraft. Eucalipto. Alcatrão.

INTRODUCTION

Gasification is a process of converting organic or fossil material into a mixture of gases having as final product H_2, CO, CO_2, N_2, light hydrocarbons (CH_4, C_2H_4, C_2H_6, etc.), among other products (ZHANG et *al.*, 2019). This technology has several applications, such as obtaining syngas that is composed of H_2 and CO, does not emit NOx-type (nitroxides) and SOy-type (sulfoxides) byproducts like fossil fuels do and does not contribute to harmful environmental effects such as acid rain (BREAULT et al., 2010; MOTTA et al., 2018; PÉREZ et al., 2023; RAJ et al., 2023).

Syngas produced by biomass gasification is an alternative fuel as it involves the conversion of organic matter such as agricultural, forestry residues or urban solid waste into combustible gas and, therefore, falls under the category of renewable energy (BURKE et al., 2018; SPEIGHT et al., 2019; SANJAYA et al., 2023). Research in renewable energy is of strategic interest to countries that are trying to detach themselves from non-renewable sources such as mineral coal, fossil fuels, and nuclear energy, as these countries do not have renewable energy as primary matrices that support internal demand (BALTHASAR et al., 2019; LIMA et al., 2020; NCHOFOUNG et al., 2023).

Before reaching the level of application as renewable energy, there are thousands of studies ranging from theoretical simulation to establish conditions to limit variables based on experimental data to kinetic and thermodynamic studies (HE et al., 2023; MARCANTONIO et al., 2023; WU et al., 2023). Kinetic studies results seek to understand the interactions between the phases involved (gas, solid and liquid), residues and their structures to describe which factors are most likely to occur to establish reaction conditions (BOCKHORN et al., 2018; GE et al., 2023).

Part of the energy generated by combustion that is not consumed in pyrolysis is used for drying in the batch portion at the beginning of the gasification process (SUSASTRIAWAN et al., 2017). Theoretical simulations propose alternative ways of analyzing specific gasification reactions to improve gas composition and performance (YANG et al., 2023; QIN et al., 2024). As result, systems with controlled operational parameters for these specific reactions have been proposed, as well as more efficient catalysts (CHEN et al., 2015; QASIM et al., 2023.; MURUGAN et al., 2024).

There is no way isolating of reactions under real operating conditions, and there are no reaction markers to monitor and estimate the contribution of each reaction to gasification. However, it is possible to get an idea of which reactions are favored by analyzing the data on the gases generated, waste (water, ash and coal and tar) generated to support kinetic and thermodynamic studies. After these studies, it's necessary to analyze which physical characteristics of equipment (reactor) can influence reactions (GAO et al., 2023). An example of a downdraft gasification reactor is shown in (Figure 1).

Figure 1 – Downdraft gasifier and temperature zone's diagram.

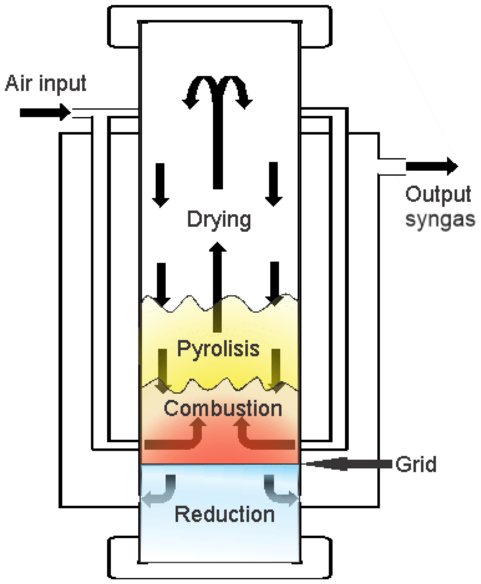

The gasification process in the reactor using the gasifying agent (air) takes place in four stages. The combustion, also called oxidation stage the air inserted into the reactor through the inlets above the grate burns the fuel (biomass) and, this generated heat provides energy to the system (CHEN et al., 2024). The drying stage takes place in the initial moments when the water of hydration of the biomass is extracted during devolatilization (KUMAR et al., 2019).

The amount of oxygen introduced into the downdraft gasifier must be lower than the stoichiometric amount required for complete combustion. (MURUGAN et al., 2023). The introduction of a lower amount of oxygen allows for the consistent formation of gas with calorific value (CO, CH_4 and H_2), and assurance that after combustion all the oxygen present in the reactor has come from the devolatilization of biomass (REED; DAS, 1988; TEZER et al., 2022). This ensures the absence of oxygen to satisfy the pyrolysis condition after the combustion region. Part of the energy generated by combustion in the initial stages of the gasification process is consumed in drying the biomass contained in the reactor (GE et al., 2023).

Pyrolysis in the downdraft gasifier is also called flaming pyrolysis, because the gas flow resulting from pyrolysis is forced to pass through the oxidizing region (combustion) of the downdraft gasifier a second time to exit the reactor, due to the structural configuration of the gas outlet being below the grid. At this stage, around 80% of the gases have been generated, the rest occurring in the reduction stage, also known as gasification, which is just below the grate (REED; DAS, 1988).

For the reduction stage to be favored, a complementary carbon source is needed to help remove oxygen through coal gasification, decarboxylation, and dehydration reactions (RIOS et al., 2018). The latter is one of the main reactions for formation of CH_4, CO_2, and H_2O in the reactor (BASU PRABIR, 2010). The complementary source is coal, which is retained on the grate. The flow of pyrolysis gas passes through the coal and enriches the gas that reaches the drag reduction region, generating ash (WEI *et al.*, 2021). The gases and matter that are not volatilized are transformed by endothermic reactions in the reduction region into permanent gases (H_2, CO, CO_2, CH_4, O_2, CnHm) (BASU PRABIR, 2010; BARUAH et al., 2014; WEI et al., 2021).

Among residues from biomass gasification, one of them is tar. It is a complex mixture of hydrocarbons with single or multiple aromatic rings as well as other functional groups (QUITETE et al., 2014). Tar has the characteristic of condensing at low temperatures, which intensifies when temperatures are lower than the one of condensation of water, leading to impregnation of inner walls of reactor ducts, causing duct blockage. Prolonged contact with tar leads to corrosion of the inner walls of metallic components (CAO et al., 2018).

Of the compounds that make up biomass tar, benzene and naphthalene have been identified as the most difficult molecules to reform (DIEGO et al., 2016). These molecules have been established as model molecules to represent tar and pointed out as reference for tar to reform requiring temperatures close to or above 1.073 K (QUITETE et al.,2014; MATERAZZI et al., 2014; DIEGO et al., 2016; SINGH et al., 2023).

Even though the potential for applying biomass in gasification is known, there are few references using pilot plants compared to theoretical proposals or systems that simulate gasification under controlled conditions. The use of renewable and low-value-added raw materials in the gasification process has gained attention due to achievement of chemical and energy production with low environmental impact (ALIAKBARI et al., 2021). Proposals involving parameter improvements in pilot plants to handle biomass to generate synthesis gas and analysis of experimental mishaps are scarce (CORTAZAR et al., 2019; VALIN et al., 2019; SILVA et al., 2023).

Therefore, this work focused on the study and optimization of a pilot downdraft gasification unit using air as a gasifying agent. Eucalyptus grandis chips were used as fuel. The objective is to evaluate differences in the synthesis gas produced in two predefined configurations which are with and without extension in the reactor body, analyzing the changes that cause variation in the amount of biomass batch and in the volume that the gas can occupy in the reactor.

MATERIAL AND METHODS

Biomass

A quantity of 100 kg of *Eucalyptus grandis* was provided by Embrapa Florestas to form chips. A 0.5 kg of this material was processed in a ball mill and passed through a 12 Tyler sieve. 0.3 Kg of the eucalyptus was used for immediate analysis (ash, volatile matter and fixed carbon). The moisture content was determined by gravimetry in a Quimis oven using the Bc 2-49 (1990) AOCS method. The ash content was determined in a Solid Steet oven using the ABNT NBR 16586:2017 method. The calorific value was determined in an IKA C200 calorimetric pump using the ASTM D 4809 method.

1 g of eucalyptus was used for the elemental analysis using CHNS FlashSmart equipment with BBOT standard oven using the ASTM D 5373 method. The higher calorific value (HHV) of the biomass was determined in reaction with oxygen in a calorimetric pump following the ASTM D4809 method.

Calculations

The determination of oxygen in elemental analysis occurs by balancing elements and components as represented in Equation 1 (BASU PRABIR, 2010).

$$\%O = 100\% - (C + H + N + S) - \%ash - \%moisture \tag{1}$$

The fixed carbon content (FC) is determined from the equation containing moisture (M), volatile matter (VM), and ash as represented in Equation 2 (BASU PRABIR, 2010).

$$FC = 100\% - M - VM - ash \quad (2)$$

The Lower Heating Value (LHV) of biomass is determined from the higher heating value (HHV), percentage of hydrogen (H), percentage of moisture (M), and latent heat of water vaporization (h_g = 2260 kJ/kg at 373,15 K) in Equation 3 (BASU PRABIR, 2010).

$$LHV = HHV - h_g\left(\frac{9H}{100}\right) - \left(\frac{M}{100}\right) \quad (3)$$

Based on a representative molecular formula for biomass as CxHyOz, and the percentage quantities obtained in the elemental analysis for carbon (x), hydrogen (y) and oxygen (z) it is possible to represent combustion of biomass as shown in Equation 4 (EMAMI-TABA et al., 2013).

$$C_xH_yO_z + \left(x + \frac{y}{4} - \frac{z}{2}\right)(O_2 + 3.76N_2) \rightarrow xCO_2 + \frac{y}{2}H_2O + 3.76\left(x + \frac{y}{4} - \frac{z}{2}\right)(N_2) \quad (4)$$

A rotameter attached to the gasifier inlet allows the volume per minute of air injected into the system to be adjusted. The measured volume is determined by the rate ($\boldsymbol{v}_{air}$) of injection in liters per minute and subsequent conversion in Nm^3/h represented in equation 5.

$$V_{air} = v_{air}\Delta t \quad (5)$$

The equivalence ratio (Φ) is a parameter that relates the quantity of air inserted into the gasifier (m_{air}) and the stoichiometric quantity of air ($m_{air_{stoich}}$) for the complete combustion of one gram of biomass, as represented in equation 6 (BASU PRABIR, 2010).

$$\Phi = \frac{m_{air}}{m_{air_{stoich}}} \quad (6)$$

The biomass consumption rate (BCR) will be calculated by the batch mass (kg) consumed per hour (Δt) as represented in Equation 7 (MA, ZHONGQING et al., 2015).

$$\mathrm{BCR} = \frac{\mathrm{m_{batch}}}{\Delta \mathrm{t}} \tag{7}$$

The gas production rate (GPR) estimates the amount of gas produced by the ratio between the volume of gas generated per hour in $\mathrm{Nm^3/h}$ (v_{output}) and the amount of mass consumed (m_{batch}) in that period. For a downdraft gasifier, the batch mass is used as represented in Equation 8 (GAI; DONG, 2012).

$$\mathrm{GPR} = \frac{\mathrm{v_{output}}}{\mathrm{m_{batch}}} \tag{8}$$

The carbon conversion efficiency (CCE) is estimated by correlating the percentage carbon-containing gas components (CO, CO_2 and CH_4) in the synthesis gas (C_{gas}) by the percentage carbon in the eucalyptus chips ($C_{eucaliptus}$). The CCE representation is shown in equation 9 (WANG et al., 2023).

$$\mathrm{CCE} = \frac{\mathrm{C_{gas}}}{\mathrm{C_{eucaliptus}}} \mathrm{x100} \tag{9}$$

The lower heating value (LHV) of the synthesis gas is estimated by the ratio between the lower heating value (LHV) of the components H_2, CO and CH_4 by the average percentage by volume obtained in the temperature range considered optimal for gasification, represented in equation 10 (PROTO et al., 2016).

$$\mathrm{LHV_{gas}} = \frac{12.622\mathrm{CO}+10.788\mathrm{H_2}+ 35.814\mathrm{CH_4}}{100} \tag{10}$$

The efficiency of cold gas (ECG) is estimated by the ratio of lower heating value of gas (LHV_{gas}) to gas production rate (GPR) by the lower heating value of biomass represented in Equation 11 (RABEA et al., 2021).

$$\mathrm{ECG} = \frac{\mathrm{LHV_{gas}GPR}}{\mathrm{LHV}} \mathrm{x100} \tag{11}$$

Experimental Setup

A pilot plant of a fixed-bed downdraft gasifier was machined from carbon steel to have a capacity of 2.2 kg of biomass. The body of the pilot plant has internal diameter of 10 cm and total height of 136 cm. Air injection point is fixated right above the grid, longitudinal fixed wells for temperature measurement that reaches the center of the reactor, the first well fixed 3 cm above the grid, other wells every 10 cm from it, and the measurement well on the flange with 30 cm long as shown in Figure 2. In the plant diagram of Figure 2, the numbering of components and instrumentation are described in Table 1.

Figure 2 – Representation of the pilot gasifier with instruments and component numbering.

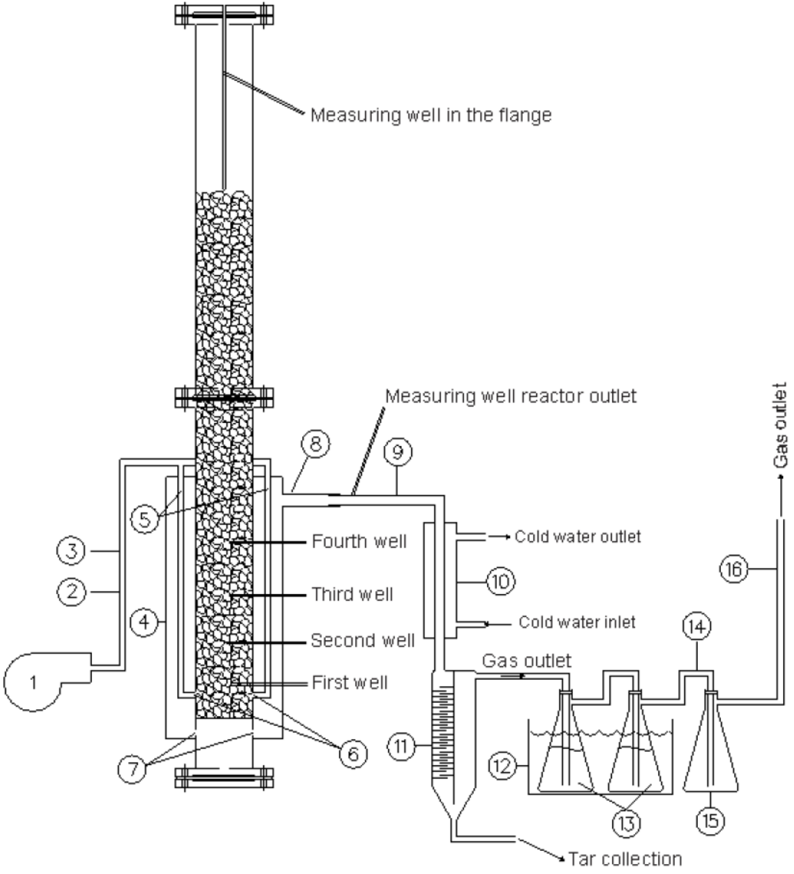

Table 1 – Numbering, and components of the pilot gasifier plant.

Number	Components
1	Compressor
2	Flow Integrator
3	Pressure Integrator
4	Reactor jacket

5	Air injection pipe
6	Air inlet to the reactor bed
7	Gas outlet pipe inside the reactor jacket
8	Unification of the gas outlet pipe in the reactor jacket
9	Pressure Integrator
10	Heat Exchanger
11	Particle Separator
12	Ice bath
13	Bubblers
14	Volume Integrator
15	Dry accumulator container
16	Analytical Integrator (GC-TCD)

A data logger receives data from thermocouples and records it versus time in graphical form. The synthesis gas generated is cooled by a heat exchanger to condense the tar and isopropanol is bubbled to remove any tar particles from the gas. A gas diffuser (not shown) directs a fraction of the synthesis gas to the detection system (GC-TCD) and the rest for disposal.

The feed conditions established were: 0.6 kg batch of Group B biomass, as described in Table 2, and an inlet air rate of 15 Nm^3/h. Pressure was a non-controllable variable, being dependent on other parameters and interferences.

Detection System (GC-TCD)

Detection starts in the gas chromatograph (GC) after the top flange is sealed. A diffuser directs a fraction of the synthesis gas to the GC, which performs 10 determinations. The GC used was a Varian CP3800 with a thermal conductivity detector (TCD) using a Carboxen 1010 column to determine the compounds CO_2, CO, H_2 and N_2 and a second Varian CP-Sil 5GB capillary column with an FID detector to detect CH_4 and light hydrocarbons. The gas flow rate in the column was set at 3.5 mL/min and the TCD temperature was set at 503 K.

Helium was used as carrier gas. Starting and maintaining the column temperature at 333 K for three minutes. In a 303 K/min ramp, the column was heated to 393 k and remained there until the determination was complete. Total elution time was eight minutes, with seven determinations per hour.

RESULTS AND DISCUSSION

Evolution of Pilot Plant

The pilot plant went through two stages of development. The first version of the equipment on study the implementation of a downdraft unit using fine branches (eucalyptus twigs) to generate synthesis gas. In this version, ignition took place through the open bottom flange with the aid of an electric blower with the batch previously loaded for subsequent sealing of the bottom and top flanges. Changes were added to this first version, such as reduction of the measuring well on the upper flange, measuring wells fixed to the reactor and extension to the reactor, changing the responses and monitoring of the gasifier, reaching the so-called second version, as shown in Figure 3.

Figure 3 - a) upper flange with 30 cm measuring well; b) reactor with measuring wells; c) reactor extension; d) assembled reactor.

The second version involved optimizing the equipment parameters and studying the influence of these parameters on gasification phenomena. Ignition began to be carried out on a 0.12 kg portion of eucalyptus through the upper flange. After burning the eucalyptus portion, average temperatures are recorded at around 1.173 K and the batch is loaded, and the top flange sealed.

Due to the structural characteristics of the reactor body, it was not possible to insert a measurement well in the reduction zone. The gas outlet ducts are 3 cm below the grate and the reactor's insulating jacket covers up to 6 cm below the grate. The extension inserted into the reactor to increase the reactor's load capacity was coated together with the reactor by a ceramic fiber blanket composed of silica and aluminum foil. After sealing the upper flange, recording data began: temperature, flow rate at the reactor inlet and outlet, and average pressures at the reactor inlet and outlet. The gas produced is determined by a GC attached to the reactor outlet.

Biomass Characterization

The 100 kg of eucalyptus chips were sorted through sieves in the 35.7 to 5.6 mm range, and the selected portions were treated statistically using the Quartile method. The method takes into account the variability in the particle size distribution of eucalyptus. The chips retained on the 16 mm sieve represent the median (Md) and are called Quartile 2 (Q_2). Quartile 1 (Q_1) is the sum of the chips from groups C and D. Quartile 3 (Q_3) is the sum of chips from groups B and A. The sieves, meshes, weight and groups selected are shown in Table 2.

Table 2 - Biomass classification per Mesh, mass and Quartile grouping.

Sieve	**Mesh (ABNT - TYLER)**	**Mesh (mm)**	**Selected biomass range (g)**	**Quartile of sifted bands**	**Group**
1	1.1/2”	35.7	120	Q_3	A
2	1.1/4”	31.5	78		
3	1”	25	252		B
4	3/4"	19	427		
5	5/8”	16	268	$M_d = Q_2$	M_d
6	1/2"	12.5	389	Q_1	C
7	3/8”	9.5	254		
8	3.1/2”	5.6	203		D
-	<3.1/2”	<5.6	212		
			$\sum = 2.203$		$E = \sum_{(group)}$

Each of group’s A to D were used separately as fuel in the gasifier studies. Group B chips were selected as optimized particle size for this study because they provide high combustion temperatures and low pressure drop in the reactor. A portion of this biomass range was characterized according to ABNT and ASTM standards and the results are shown in Table 3.

Table 3 - Analysis for biomass characterization.

Analysis	**Symbol**	**Result**
Elemental Analysis		
Carbon	C	43.68 (%)
Hydrogen	H	5.26 (%)
Nitrogen	N	0.20 (%)
Sulfur	S	0
Oxygen	O	41.70 (%)
H/C		0.12

O/C		0.95
Immediate Analysis		
Moisture Content	M	8.81 (%)
Ashes	ASH	0.35 (%)
Volatile Material Content	VM	0.37 (%)
Fixed Carbon	FC	90.47 (%)
Higher Heating Value	HHV	17.39 (MJ/kg)
Lower Heating Value	LHV	16.52 (MJ/kg)

With data from elemental analysis of eucalyptus for C H, N and S, the percentage value of 41.70% was calculated for oxygen, according to equation 1, and the H/C correlations were 0.12 and O/C 0.95. According to the Van Krevelen diagram, the higher the H/C value and the lower the O/C value, better is the solid fuel.

The results of the elemental and immediate analysis of eucalyptus chips do not represent good results as a solid fuel when compared to mineral coal, as they have lower values (WANG *et al.*, 2020). However, eucalyptus is a renewable material, so it can be produced in short time cycles and in quantities that compensate for the low quality of eucalyptus as a solid fuel (BALAEVA et al., 2015; APRIANTI et al., 2023).

The immediate analysis determined a low value of 0.37% for VM in eucalyptus, which directly affects the gasification process that has the volatilized lignocellulosic material as a reactant in gasification. The LHV value of 16.52 MJ/kg calculated according to equation 3 is half the energy value when compared to the average values for mineral coal of 36 MJ/kg, for example. The low value for M at 8.81% mitigates the disadvantage of the eucalyptus chips used, as less heat is required in the devolatilization process (KOMILIS et al., 2014).

The calculated FC of 90.47% is a characteristic that is influenced by VM. Values of 90% correspond to how well the eucalyptus burns to form charcoal in the combustion stage. The correlation between CF and ash content of 0.35% indicates that the eucalyptus chip sample may have a good conversion of carbon into gas.

Gasifier Operating Parameters

Optimization of the pilot plant for the configurations with and without extension was carried out according to the following requirements: profile temperatures with lower oscillations for the oxidizing region, higher temperature levels for the oxidizing region, and longer gasification operating time. The pressure was a non-controllable variable, depending on other parameters such as the air flow rate and interference as the deposition of waste in the ducts at the reactor outlet.

In the configuration with an extension on the reactor, average inlet pressures ranging from 0.30 to 0.45 bar and outlet pressures ranging from 0.25 to 0.30 bar were observed; in the configuration without the extension, average inlet pressures ranged from 0.5 to 0.80 bar and outlet pressures ranged from 0.45 to 0.65 bar. The gasifier's operating data: air flow rate. outlet gas flow rate. biomass consumption rate (BCR) and the gas production rate (GPR). The results are described in Table 4 below.

Table 4 - Details of eucalyptus gasification in Downdraft Fixed Bed Gasifier.

Runs		**Output gas (m^3/h)**	**BCR (Kg/h)**	**GPR (Nm^3/Kg)**
With extension on the reactor	1	1.30	2.60	0,71
	2	1.25	2.40	0,76
	3	1.27	2.40	0,69
No extension on the reactor	1	1.28	2.30	1.11
	2	1.05	2.40	0.68
	3	1.59	2.43	1.48

The average quantities of waste collected per triplicate in both configurations: coal (over the grate), ash (under the bottom flange), and tar shown in Table 5.

Table 5 - Average quantities collected of water, coal, ash and tar.

Configuration	**Water (mL/Kg)**	**Coal (g/Kg)**	**Ash (g/Kg)**	**Tar (g/Nm^3)**
With extension on the reactor	157	22.30	1.67	0.80
No extension on the reactor	153	36.70	3.34	1.55

Temperature Profiles

The temperatures of the runs in the configurations with and without extension in the reactor for 80 minutes were recorded in a data logger. The temperature profiles showed a decreasing gradient, where the highest temperature point is in the oxidation stage (near the grate) and the lowest is in the measurement well on the upper flange, as there is no biomass near it. Sharp oscillations were observed in the curves (Figures 5 and 6) at the most oxidizing points due to the inhomogeneous flow of the eucalyptus chips inside the reactor.

There is intense devolatilization with release of water vapor, oily lignocellulosic extract and part of volatile organic compounds in the first 10 minutes of running in the extended configuration. When this lignocellulosic oily extract is not consumed, it reaches regions of low temperatures, impregnating the internal walls of the reactor and chips that have not yet been consumed. The temperature profile of the triplicate in the configuration is shown in Figure 5.

Figure 5 - Temperature records and distinction of the average temperature at the most oxidizing points in the first 35 min. First black. second red. third blue. thermocouple on flange in magenta. thermocouple at reactor outlet in green.

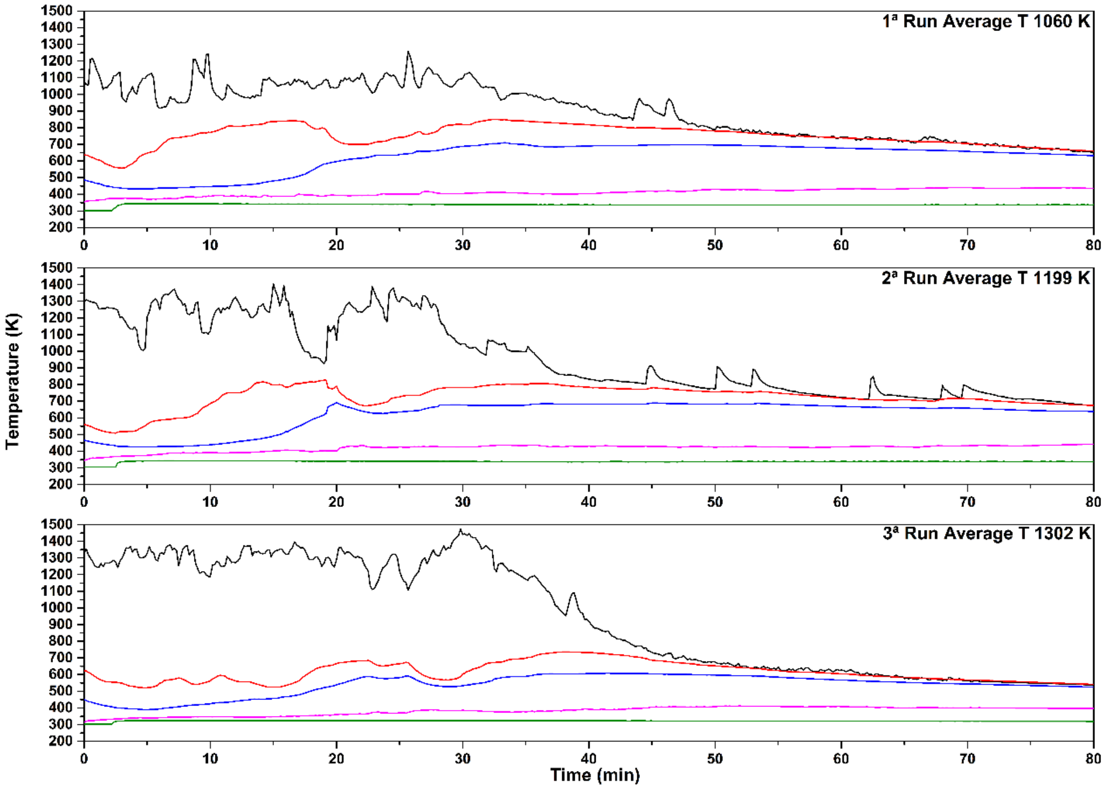

In the temperature profiles shown in Figure 5, the first 35 min were considered the optimum temperatures, as these are the temperatures at which the reforming of benzene and naphthalene occurs at average temperatures of 1060 K (1ª run), 1199 K (2ª run) and 1302 K (3ª run). After this optimum maximuns there is a decrease in temperature as response to depletion of eucalyptus chips in the reactor bed. These average temperatures meet the conditions for tar reforming in flaming pyrolysis, which manages to reform most of the volatile organics in the reactor before reaching the reduction region (REED; DAS, 1988).

In runs 1ª, 2ª and 3ª, between 35 and 70 min, temperatures ranging from 1060 to 573 K were recorded in the second measuring well. Some authors point out that in the temperature range above 400 °C there are reform conditions for tar (MATERAZZI et al., 2014; FRAINETTI et al., 2023; SINGH et al., 2023).

The extension in the reactor increased the volume to be occupied by the gas. The distance from the oxidizing region cools the gas, which generates an average temperature gradient of 1173 to < 373 K. Keeping the gas warm requires a great amount of heat, and therefore decreases the energy to carry out flaming pyrolysis and reduction (TEZER *et* *al*., 2022). The last curve (green line) in runs 1ª, 2ª and 3ª refers to the measurement well in the flange of the reactor with temperatures below 373 K. The penultimate (magenta line) records in runs 1ª, 2ª and 3ª refer to the measurement well at the reactor outlet with temperatures below 413 K, shown in Figure 6.

Figure 6 - Thermocouple temperature records and distinction of the average temperature at the most oxidizing point in the first 25 minutes. First black. second red. third blue. thermocouple on flange in magenta. thermocouple at reactor outlet in green.

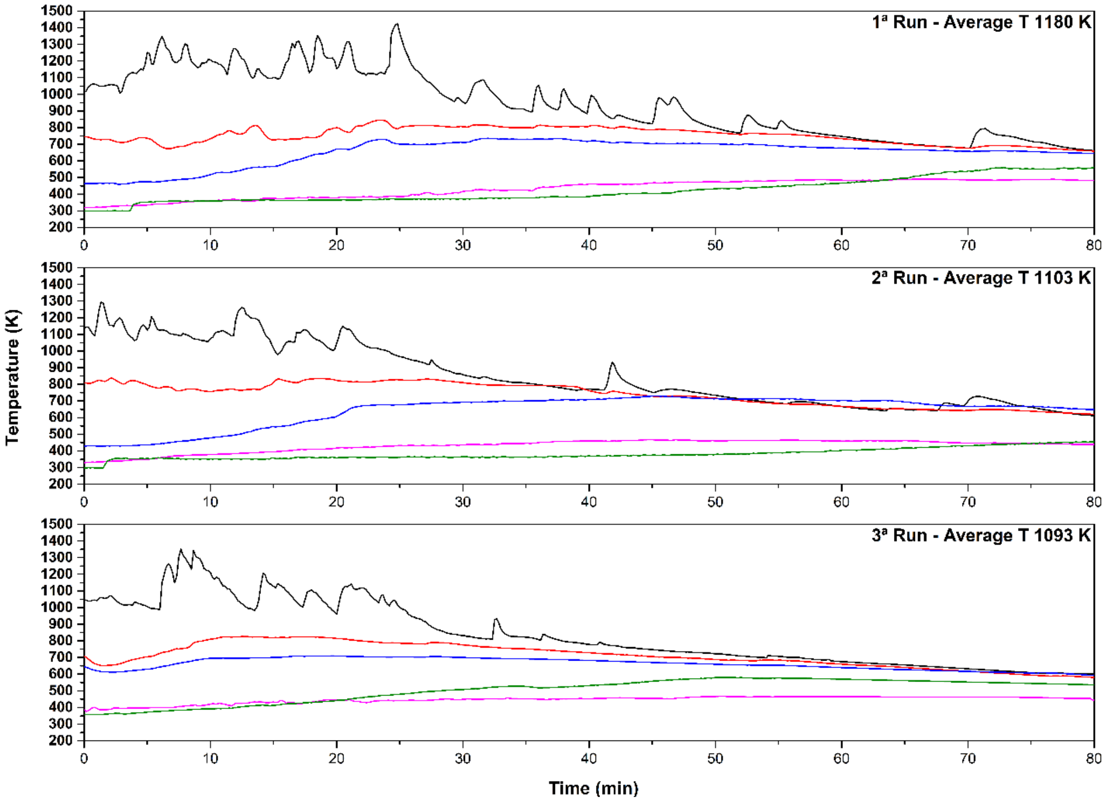

In the condition without extension in the reactor, the temperatures considered optimal for the reforming of benzene and naphthalene occurred up to 25 min with average temperatures of 1.180 K (1ª run). 1.103 K (2ª run), and 1.093 K (3ª run). In runs 1. 2 and 3. a slight decrease was observed in the first five minutes due to intense devolatilization. In the second fixed measurement well, between 25 and 70 min, the temperatures ranged from 1.093 to 623 K, so the temperatures were higher than those observed in the configuration with extension.

The last curve (green line) in runs 1ª, 2ª and 3ª in the configuration without extension is the fixed measurement well in the reactor flange with temperature records reaching 573 K. An average temperature gradient was observed between 1.123 and 573 K and was therefore lower than that observed in the configuration with extension. The value was lower at the maximum and higher at the minimum temperature gradients. The penultimate records (magenta line) in runs 1ª, 2ª and 3ª, the fixed well at the reactor outlet recorded temperatures of up to 573 K because there was no excessive heat loss to the reactor walls.

Gases Generated in Gasification

The synthesis gas was analyzed using gas chromatography, and the gaseous products were H_2, N_2, CO, CH_4 and CO_2. The determinations in the configurations with and without extension in the reactor were compiled in %mol/mol concentration and presented in Table 6.

In the configuration with reactor extension there was low production of H_2 and CH_4. So, two of the gases that contain heating value were not produced in most of the runs (MANKASEM et al., 2024). According to Mankasem et al., (2024), at temperatures below 673 K, the material deposited on the reactor's inner walls is not completely consumed and remains adhered to the walls after the cooling stage. In regions of the reactor where the temperature fell below 373 K, volatile organic compounds condensed on the inner walls of the reactor extension.

This phenomenon is reflected in the amount of tar retained at the collection point described in Table 5. The lignocellulosic material deposited on the inner walls of the reactor and extension leads to a situation in which a significant part of the volatile organic material is not reformed in the flaming pyrolysis and therefore affects the conversion into permanent gas in the reduction region (REED; DAS, 1988). Excess heat was also lost to the internal walls of the reactor and the extension, as seen in the decrease in order of temperature values recorded by the second and third fixed measuring wells shown in Figure 7.

Table 6 – Triplicate determinations of eucalyptus biomass in the configuration with and no extension in the reactor.

Configuration with extension on the reactor

H_2(%mol/mol)			**N_2(%mol/mol)**			**CO(%mol/mol)**			**CH_4(%mol/mol)**			**CO_2(%mol/mol)**		
1ª Run	**2ª Run**	**3ª Run**	**1ª Run**	**2ª Run**	**3ª Run**	**1ª Run**	**2ª Run**	**3ª Run**	**1ª Run**	**2ª Run**	**3ª Run**	**1ª Run**	**2ª Run**	**3ª Run**
0.885	6.632	7.372	51.465	52.089	46.016	9.730	9.264	14.301	1.595	0.462	1.004	13.938	13.535	10.733
			52.352	55.679	52.689	8.394	6.882	7.015	1.476	0.301	0.832	13.671	13.638	12.883
			51.617	58.473	55.604	9.655	4.258	4.355	1.336	0.180	0.568	14.305	14.793	16.202
			59.442	39.223	55.060	4.608	16.072	6.914	0.315	3.932	0.311	15.182	11.716	13.196
			58.676	58.579	59.058	2.636	1.984	2.951	0.383			15.312	15.113	15.198
			59.576	52.679	53.141	1.512	0.871	0.968				14.937	9.051	10.204
			51.669	51.894	48.719	0.888	0.786	0.584				8.944	6.525	4.620
			55.690	48.196	48.225	1.029	0.688	0.857				13.025	4.599	4.708
			51.110	53.806	49.843	1.212	1.998	0.705				8.710	10.959	2.893

Configuration no extension on the reactor

H_2(%mol/mol)			**N_2(%mol/mol)**			**CO(%mol/mol)**			**CH_4(%mol/mol)**			**CO_2(%mol/mol)**		
1ª Run	**2ª Run**	**3ª Run**	**1ª Run**	**2ª Run**	**3ª Run**	**1ª Run**	**2ª Run**	**3ª Run**	**1ª Run**	**2ª Run**	**3ª Run**	**1ª Run**	**2ª Run**	**3ª Run**
4.164	4.179	2.230	60.476	53.368	66.527	8.693	6.835	2.644	0.260	1.223	0.320	14.490	8.276	18.034
8.395	2.376	2.366	49.119	66.916	67.096	14.877	3.506	3.492	3.281	0.319	0.263	11.795	16.416	17.263
2.078	1.404	4.018	66.134	63.047	62.030	4.144	2.122	8.417	0.323	0.326	0.629	17.686	15.235	14.865
		1.565	62.035	58.128	66.580	1.393	1.559	2.354	0.296	0.251	0.238	14.647	9.724	17.461
1.439	22.211		62.936	58.134	62.102	2.467	2.116	1.359	0.809	0.293	0.210	16.526	10.144	14.662
			55.755	55.593	55.683	1.245	1.489	0.968	0.400	0.246	0.211	7.783	4.908	7.097
			55.776	55.842	58.559	1.093	1.356	1.044	0.424	0.219	0.203	6.004	3.775	10.173
18.176		1.474	55.077	55.429	53.840	0.926	0.940	0.851	0.489	0.194	0.201	2.930	3.076	4.051
10.429		2.089	55.177	54.578	57.666	0.977	0.604	2.154	0.472	0.195	0.388	2.846	1.421	9.351

Excess heat was also lost to the internal walls of the reactor and the extension, as seen in the decrease in order of temperature values recorded by the second and third fixed measuring wells shown in Figure 7.

Figure 7 - a) Inner wall of the reactor with markings at 4 and 10 cm upward from the fourth fixed measurement well and material deposited; b) Inner appearance of the extension with deposits of devolatilized material.

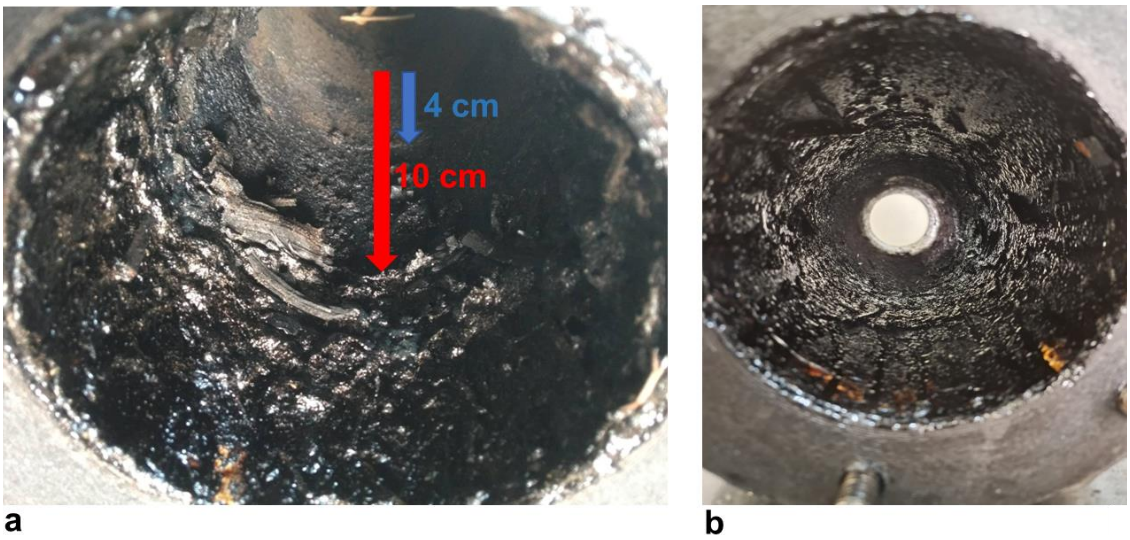

Figure 7 (a) shows that there is no material deposited on the walls of the reactor up to a height of 37 cm from the grate, as the heat generated during combustion and the flaming pyrolysis have managed to consume all the material. Moving further away from the grate, it’s seen a gradual deposition on the inside walls of the reactor. From a height of 43 cm from the grate up to the connection between the reactor and the reactor extension that housed the eucalyptus chips, there was a severe deposit of unconsumed charcoal and condensed material.

Figure 7 (b) shows the devolatilized material and condensed volatile material originating from gas impregnated in the inner walls of the reactor extension. In this configuration, H2 was only detected in the first GC determination, and methane was partially produced in the first four determinations using the reactor extension. The analysis of Φ, described in Table 4, allows us to conclude that Φ was not responsible for this limitation in gas production, as there was no significant change in the values in the triplicate.

In the configuration without extension in the reactor, the gas was not subjected to temperatures lower than 573 K, which reduced the losses of material deposited on the internal walls of the reactor and reduced the heat losses to the walls of the extension and to the heating of the gas. Under these conditions, methane was detected in all determinations, so all reactions involving CH_4 were affected (GÓMEZ *et al*., 2023). H_2 was detected in almost all the determinations except the seventh and eighth, and no changes were observed in the behavior of the gasifier to justify this non-detection. The main products of incomplete combustion in biomass gasification are CH_4 and H_2 (BASU PRABIR, 2010).

Gasifier Performance

The performance of the gasifier was assessed using a set of parameters: lower heating value (LHV) of gas, which estimates the amount of heat contained in the sum of lower heating values of the H_2, CO and CH_4 components; carbon conversion efficiency (CCE), which estimates how much of carbon originating from the biomass is converted into a gaseous product; and cold gas efficiency (CGE), which estimates potential energy of gas leaving the gasifier based on heating value of the biomass.

The performance of the gasifier was calculated with the data extracted within the optimum reforming range until 35 min for the configuration with extension and 25 min for the configuration without extension, based on equations 10, 9, 11 and 6. The average percentages of the gaseous components H_2, N_2, CO, CH_4 and CO_2 obtained in this optimum temperature range are shown in Table 7.

Table 7 – Average performance of the Gasifier System.

Runs		**Φ**	**CCE (%)**	**LHV$_{gas}$ (MJ/ Nm^3)**	**ECG (%)**	**%H_2**	**%N_2**	**%CO**	**%CH_4**	**%CO_2**
with extension on the reactor	1ª	0,29	69.69	1.99	8,.5	1.14	68.42	10.49	1.53	18.42
	2ª	0,28	68.09	3.19	14.68	11	59.26	11.64	1.50	16.60
	3ª	0,29	66.19	2.66	11.11	9.28	61.81	10.60	0.89	17.42
no extension on the reactor	1ª	0,26	61.47	2.17	14.58	5.54	67.61	8.31	1.47	17.07
	2ª	0,15	43.43	0.96	3.95	3.34	77.69	2.76	0.70	15.51
	3ª	0,26	54.92	1.05	9.41	2.83	73.18	4.71	0.41	18.87

The equivalence ratio (Φ) is a parameter that affects carbon conversion and gasifier performance, especially when the gasifying agent is air, and depends on the characteristics of the biomass and the type of gasifier (PROTO et al., 2016; CHAVES et al., 2023). According to Basu (2010), rates above 0.27 tend to convert almost all phenols and reduce tar formation during gasification. For Φ values significantly below 0.20 result in a series of problems such as incomplete gasification, excessive char formation and a low heating value of the gaseous product. Values of Φ above 0.40 tend to result in complete combustion and the formation of CO_2 and H_2O as the main product. In the literature, there are studies on gasification that point to Φ in the range of 0.20 to 0.35 as having positive results depending on the conditions of the raw material and equipment (GUO et al., 2014; SALES et al., 2017; KUMAR et al., 2022). Under the conditions used in this study, the air injection parameter optimized at 15 L/min provided an Φ in the range 0.26 to 0.29. It was observed that the second run in the configuration without extension worked with Φ at 0.15, due to the pressure drop at the reactor outlet detected by the rise in pressure recorded on the manometer.

The extension in the reactor increased the volumetric capacity, affecting the performance of the gasifier in two fundamental respects. Firstly, combustion did not generate enough heat to supply the process and keep all the gas heated above the 43 cm height of the bed in relation about the grate, at temperatures above 673 K. Secondly, the increase in the reactor's internal volume eased the pressure in the system. The extra volume provided by the extension temporarily accommodated the gas generated, which allowed the gas to flow through the reactor's outlet ducts without increasing the pressure too much. This behavior is similar to that reported in the Venturi tube. The increased flow in the ducts causes the material deposited on the internal walls of these ducts to be dragged along, accumulating in spots and aggravating the pressure drop. Lower pressure ranges at the reactor outlet result in lower pressure drop at the reactor outlet, and therefore greater homogeneity of the gas flow and lower pressure at the system inlet.

When comparing the CCE, LHV and ECG performance parameters for the configurations with and without extension, the configuration with extension performed best. Regarding the gaseous products H_2, CO, CH_4 and CO_2, the configuration with extension in the reactor obtained an average yield of 54.65% for H_2, 48.21% for CO, 65.65% for CH_4 and 5.72% for CO_2. Therefore, the configuration with reactor extension was the optimized configuration for the second version of the pilot plant.

The optimized condition of the second version of the pilot plant was compared to the studies in the literature that used downdraft fixed bed pilot plants with air as the gasifying agent and eucalyptus and various woods as fuel, as shown in Table 8.

Table 8 - Performance evaluation using the parameters Φ, CCE, LHVgas and ECG percentages of the gaseous products H_2, CO, CO_2 and CH_4.

Biomass	**References**	**Φ**	**CCE (%)**	**LHV_{gas} (MJ/ Nm^3)**	**ECG (%)**	**%H_2**	**%CO**	**%CO2**	**%CH_4**
Eucalyptus	(Autor)	0.29	69.69	1.99	8.5	1.14	68.42	10.49	1.53
		0.28	68.09	3.19	14.68	11	59.26	11.64	1.50
		0.29	66.19	2.66	11.11	9.28	61.81	10.60	0.89
Eucalyptus	(CHAVES *et al.*, 2023)	–	89	5.77 to 6.77	–	15.13	22.86	13.49	4.67
	(KUMAR *et al.*, 2022)	0.309 to 0.399	–	3.02 to 3.709	–	10.80 to 12.40	10.10 to 13.30	9.20 to 10.70	0.90 to 1.30
	(SALES *et al.*, 2017)	0.396 to 0.492	–	7.13 to 8.35	75	16 to 17.40	16.90 to 21.20	–	1.20 to 1.80
Danish pine	(RAHMAN *et al.*, 2021)	0.27 to 0.41	–	4.57 to 5.11	75.40 to 93.10	15.90 to 20.60	16.30 to 25.60	7.10 to 11.80	0.44 to 1.03
Mahua	(RAJ *et al.*, 2023)	0.43	–	3.978	38.42	17.55	22.16	11.89	3.07
Mimosa	(BUNCHAN *et al.*, 2017)	–	35.30	3.82 to 3.9	34.01 to 35.36	6.75 to 8.47	13.86 to 16.33	5.73 to 13. 53	2.97 to 3.64

Comparing the results of the configuration with reactor extension with those found in the literature, listed in Table 8, for the gasifier performance parameters, it was observed that the value found for CCE was lower than that of Chaves *et al.*, (2023), and higher than that of Bunchan *et al.*, (2017), the other studies did not calculate the carbon conversion rate. For the LHV parameter of the gas, this work obtained a value in the same range obtained by Kumar et al., (2022), being lower than the other works for the lower heating value. For the ECG parameter, the value found was lower than that of Sales et al., (2017), that of Rahman et al., (2021), that of Raj et al., (2023), and that of Bunchan et al., (2017), other studies did not calculate the efficiency of cold gas. The comparison between the percentages of gaseous products showed that the concentration of H_2 was higher only in relation to Bunchan et al., (2017), while it was lower in relation to all studies Rahman et al., (2021), and Raj et al., (2023), for concentrations of CO, CH_4. The concentration of CO_2 in this study was higher than all comparative references.

CONCLUSION

The insertion of the extension to the reactor subjected part of the gas and part of the volatile material to temperatures lower than those required for reforming the tar, which consequently deposited organic material on the internal walls and caused heat loss. The inhomogeneity of the eucalyptus chip flow inside the reactor bed and the gas flow at the reactor outlet was observed, due to the loss of load caused by tar, blocking the outlet ducts.

The optimized condition occurred with the configuration with extension in the reactor using eucalyptus chips. It recorded average temperatures above 1073 K, average production of 1.29 m^3/h of gas, and gas fractions of 7.14% H_2, 10.91% CO, 1.31% CH_4 and 17.48% CO_2. The performance of CCE, LHV and ECG in the reactor extension configuration were respectively 21.68%, 40.46% and 8.28%. These values were higher on average than the results obtained in the configuration without extension in the reactor.

The second version of the pilot plant provided satisfactory conditions for the study of the parameters that influence the downdraft fixed bed gasifier and indications of which reactions were favored. With the data generated in this second version, proposals were made for improvements which, when implemented, will make up the third version of the pilot plant. However, the performance of the pilot plant version 2.0 about the works found in the literature was inferior. There is room for improvement. These improvements could include: operating only in the configuration without extending the reactor, using the maximum capacity of 0.4 kg per run to accommodate the biomass in the region of complete removal of material from the internal walls, adding a semi-continuous feeder on the upper flange of the reactor for 24 hour operation, including a fixed measuring well in the reduction region, adding a device for removing ash, increasing the flow rate of the ducts at the gas outlet to minimize the pressure drop.

REFERENCES

ALIAKBARI, R.; GHASEMI, M. H.; NEEKZAD, N.; KOWSARI, E.; RAMAKRISHNA, S.; MEHRALI, M.; MARFAVI, Y. High value add bio-based low-carbon materials: conversion processes and circular economy. **Journal of Cleaner Production**, v. 293, p. 126101, 2021.

APRIANTI, N.; FAIZAL, M.; SAID, M.; NASIR, S.; FUDHOLI, A. Gasification kinetic and thermodynamic parameters of fine coal using thermogravimetric analysis. **Energy**, v. 268, p. 126666, 2023.

BALAEVA, Y. S.; MIROSHNICHENKO, D. V.; KAFTAN, Y. S. Predicting the classification characteristics of coal. Part 1. The gross calorific value in the wet ash-free state. **Coke and Chemistry**, v. 58, n. 9, p. 321-328, 2015.

BALTHASAR, A.; SCHREURS, M. A.; VARONE, F. Energy Transition in Europe and the United States: policy entrepreneurs and veto players in federalist systems. **The Journal of Environment & Development**, v. 29, n. 1, p. 3-25, 2019.

BARUAH, D.; BARUAH, D. C. Modeling of biomass gasification: a review. **Renewable And Sustainable Energy Reviews**, v. 39, p. 806-815, 2014.

BASU PRABIR. Biomass gasification and pyrolysis: practical design and theory. 1st ed.: **Published by Elsevier Inc**., 2010. Available in: https://www.sciencedirect.com/book/9780123749888/biomass-gasification-and-pyrolysis. Acess in: 07 jan 2024.

BREAULT, R. W. Gasification Processes Old and New: A Basic Review of the Major Technologies. **Energies**, USA, v. 3, n. 2, p. 216-240, 2010.

BOCKHORN, H. Gasification kinetics. **Underground Coal Gasification and Combustion**, p. 213-252, 2018.

BURKE, MATTHEW J.; STEPHENS, JENNIE C.. Political power and renewable energy futures: a critical review. **Energy Research & Social Science**, v. 35, p. 78-93, 2018.

BUNCHAN, S.; POOWADIN, T.; TRAIRATANASIRICHAI, K. A Study of Throat Size Effect on Downdraft Biomass Gasifier Efficiency. **Energy Procedia**, v. 138, p. 745-750, 2017.

CAO, J-P.; REN, J.; ZHAO, X-Y.; WEI, X-Y.; TAKARADA, T. Effect of atmosphere on carbon deposition of Ni/Al2O3 and Ni-loaded on lignite char during reforming of toluene as a biomass tar model compound. **Fuel**, v. 217, p. 515-521, 2018.

CHAVES, M.; TORRES, C.; TENORIO, C.; MOYA, R.; ARIAS-AGUILAR, D. Syngas Characterization and Electric Performance Evaluation of Gasification Process Using Forest Plantation Biomass. **Waste and Biomass Valorization**, p. 1-18, 2023.

CHEN, J.; TAMURA, M.; NAKAGAWA, Y.; OKUMURA, K.; TOMISHIGE, K. Promoting effect of trace Pd on hydrotalcite-derived Ni/Mg/Al catalyst in oxidative steam reforming of biomass tar. **Applied Catalysis B: Environmental**, v. 179, p. 412-421, 2015.

CHEN, Z.; LIAO, Y.; CHEN, Y. MA, X. Insight into the gas pollutants emission of rural solid waste during the gasification-combustion process: influencing factors and mechanisms. **Fuel**, v. 355, p. 129510, 2024.

CORTAZAR, M.; LOPEZ, G.; ALVAREZ, J.; AMUTIO, M.; BILBAO, J.; OLAZAR, M. Behaviour of primary catalysts in the biomass steam gasification in a fountain confined spouted bed. **Fuel**, v. 253, p.1446-1456, 2019.

DIEGO, L. F.; GARCÍA-LABIANO, F.; GAYÁN, P.; ABAD, A.; MENDIARA, T.; ADÁNEZ, J.; NACKEN, M.; HEIDENREICH, S.. Tar abatement for clean syngas production during biomass gasification in a dual fluidized bed. **Fuel Processing Technology**, v. 152, p. 116-123, 2016.

EMAMI-TABA, L.; IRFAN, M. F.; DAUD, W. M. A. W.; CHAKRABARTI, M. H. Fuel blending effects on the co-gasification of coal and biomass – A review. **Biomass and Bioenergy**, v. 57, p. 249-263, 2013.

FRAINETTI, A. J.; KLINGHOFFER, N. B. Recent experimental advances on the utilization of biochar as a tar reforming catalyst: a review. **International Journal of Hydrogen Energy**, v. 48, n. 22, p. 8022-8044, 2023.

HE, J.; XIAO, R.; NIE, Q.; ZHONG, J.; HUANG, B. High-volume coal gasification fly ash–cement systems: experimental and thermodynamic investigation. **Construction and Building Materials**, v. 377, p. 131082, 2023.

GAI, C.; DONG, Y. Experimental study on non-woody biomass gasification in a downdraft gasifier. **International Journal of Hydrogen Energy**, v. 37, n. 6, p. 4935-4944, 2012.

GAO, Y.; WANG, M.; RAHEEM, A.; WANG, F.; WEI, J.; XU, D.; SONG, X.; BAO, W.; HUANG, A.; ZHANG, S. Syngas Production from Biomass Gasification: influences of feedstock properties, reactor type, and reaction parameters. **Acs Omega**, v. 8, n. 35, p. 31620-31631, 2023.

GE, Z.; CAO, X.; ZHA, Z.; MA, Y.; ZENG, M. Y.; HOU, Z.; ZHANG, H. Establishment of correlation between reaction kinetics and carbon structures in the char gasification process. **Carbon Resources Conversion**, v. 6, n. 2, p. 67-75, 2023.

GÓMEZ, L.; GRASA, G.; MARTÍNEZ, I.; MURILLO, R. Performance study of a methanation process for a syngas obtained from a sorption enhanced gasification process. **Chemical Engineering Science**, v. 267, p. 118291, 2023.

GUO, F.; DONG, Y.; DONG, L.; GUO, C.. Effect of design and operating parameters on the gasification process of biomass in a downdraft fixed bed: an experimental study. **International Journal of Hydrogen Energy**, v. 39, n. 11, p. 5625-5633, 2014.

KOMILIS, D.; KISSAS, K.; SYMEONIDIS, A. Effect of organic matter and moisture on the calorific value of solid wastes: an update of the tanner diagram. **Waste Management**, v. 34, n. 2, p. 249-255, 2014.

KUMAR, R. MUTHU, D.; ANAND, R. Production of biofuel from biomass downdraft gasification and its applications. **Advanced Biofuels**, p. 129-151, 2019.

KUMAR, P.; SUBBARAO, P. M. V.; KALA, L. D.; VIJAY, V. K. Real-time performance assessment of open-top downdraft biomass gasifier system. **Cleaner Engineering and Technology**, v. 7, p. 100448, 2022.

MA, Z.; YE, J.; ZHAO, C.; ZHANG, Q. Gasification of rice husk in a downdraft gasifier: The effect of equivalence ratio on the gasification performance, properties, and utilization analysis of byproducts of char and tar. **BioResources**. v. 10, n. 2, p. 2888-2902, 2015.

MANKASEM, J.; PRASERTCHAROENSUK, P.; PHAN, A. N. Intensification of two-stage biomass gasification for hydrogen production. **International Journal of Hydrogen Energy**, v. 49, p. 189-202, 2024.

MARCANTONIO, V.; PAOLA, L. D.; FALCO, M.; CAPOCELLI, M. Modeling of Biomass Gasification: from thermodynamics to process simulations. **Energies**, v. 16, n. 20, p. 7042, 2023.

MATERAZZI, M.; LETTIERI, P.; MAZZEI, L.; TAYLOR, R.; CHAPMAN, C. Tar evolution in a two stage fluid bed–plasma gasification process for waste valorization. **Fuel Processing Technology**, v. 128, p. 146-157, 2014.

MILNE, T. A.; EVANS, R. J.; ABATZAGLOU, N. Biomass Gasifier "'Tars'": Their Nature, Formation, and Conversion. Golden, CO (US): US **Department of Energy (US)**, 1998. Available in: https://www.nrel.gov/docs/fy99osti/25357.pdf. Acess in: 19 feb 2024.

MURUGAN, P. C.; KUMAR, K. V. Satheesh; DHARMARAJ, M.; RAJ, T. Prakash; PRAGADEESHWAR, K. S.; MUZAMMIL, A. K. M. Mohammed; JOSHUA, P. S.; NEDUNCHEZHIYAN, A. Experimental analysis of rice husk gasification in a newly developed air blown bed gasifier. In: **AIP Conference Proceedings**. AIP Publishing, 2023.

MURUGAN, P C; SEKHAR, S. J.; GLIVIN, G.; RAVEENDRAN, P. S.; LE, T. H. T.; MATHIMANI, T. Investigation on thermochemical co-gasification of rice husk and groundnut shell in open core gasifier for the generation of producer gas: an optimization by central composite design. **Environmental Research**, v. 242, p. 117741, 2024.

NCHOFOUNG, T. N.; FOTIO, H. K.; MIAMO, C. W. Green taxation and renewable energy technologies adoption: a global evidence. **Renewable Energy Focus**, v. 44, p. 334-343, 2023.

SILVA, L, E. E.; VIEIA, A. R.; MARTINEZ, Á. J. D.; LEITE, M. A. H.; ROCHA, M. H.; VILAS BÔAS, S. C. A.; MENDOZA, M. A. G. Gaseificação e pirólise para a conversão da biomassa em eletricidade e biocombustíveis. **Biocombustíveis. Interciência**, v. 1, p. 411-498, 2012.

PAIVA, R. C.; BORGES, L. E. P.; NORONHA, F. B. Gasification of eucalyptus in downdraft fixed bed to obtain synthesis gas. Gasification Of Eucalyptus In Downdraft Fixed Bed To Obtain Synthesis Gas, Rio de Janeiro, **Revista Militar de Ciência e Tecnologia**, v. 39, n. 2, p. 1-15, 2022.

PÉREZ, V.; BAILERA, M.; LISBONA, P. Syngas production by gasification processes. **Advances in Synthesis Gas**: Methods, Technologies and Applications, p. 17-46, 2023.

PROTO, A. R.; LONGO, L.; GAMBELLA, F.; ZIMBALATTI, G.; MACRÌ, G.; GALLUCCI, F.; CARUSO, L.; SALERNO, M.; COLANTONI, A. Energetic Characteristics of Syngas Obtained from Gasification of Hazelnut Prunings. **Procedia - Social and Behavioral Sciences**, v. 223, p. 835-840, 2016.

QASIM, M.; AYOUB, M.; SINGH, K.; INAYAT, A.; SHAMSUDDIN, R.; DANISH, M.; FARRUKH, S. A Comparative Study of Eggshell and Commercial Sorbent-Based Catalysts through Synthesis and Characterization for SESR Process. **Sustainability**, v. 15, n. 20, p. 14762, 2023.

QIN, L.; FANG, J.; ZHU, S.; ZHAO, B.; HAN, J. Municipal solid waste gasification by hot recycling blast furnace gas coupled with in-situ decarburization to prepare blast furnace injection of hydrogen-rich gas. **Waste Management**, v. 174, p. 153-163, 2024.

RABEA, K.; BAKRY, A. I.; KHALIL, A.; EL-FAKHARANY, M. K.; KADOUS, M. Real-time performance investigation of a downdraft gasifier fueled by cotton stalks in a batch-mode operation. **Fuel**, v. 300, p. 120976, 2021.

RAHMAN, M. D. M.; ARAVINDAKSHAN, S.; MATIN, M. D. A. Design and performance evaluation of an inclined nozzle and combustor of a downdraft moving bed gasifier for tar reduction. **Renewable Energy**, v. 172, p. 239-250, 2021.

RAJ, R.; TIRKEY, J. V.; JENA, P. Gasification of Briquette, Mahua wood, and Coconut shell and application to CI engines: comparative performance and optimisation analysis. **Industrial Crops and Products**, v. 199, p. 116758, 2023.

REED, T. B; DAS, A. Handbook of biomass downdraft gasifier engine systems. Colorado: **Biomass Energy Foundation**, 1988. Available in: https://www.nrel.gov/docs/legosti/old/3022.pdf. Acess in: 07 jan 2024.

RIOS, M. L. V.; GONZÁLEZ, A. M.; SILVA, L. E. E.; OLMO, O. A. A. Reduction of tar generated during biomass gasification: a review**. Biomass And Bioenergy**, v. 108, p. 345-370, 2018.

SANJAYA, E.; ABBAS, A. Plasma gasification as an alternative energy-from-waste (EFW) technology for the circular economy: an environmental review. **Resources, Conservation And Recycling**, v. 189, p. 106730, 2023.

VILAS BÔAS, S. C. A. P.; MAYA, D. M. Y.; SILVA, L. E. E.; LESME, J. R.; REYES, A. M, M.; GONZÁLEZ, A. M.; ANDRADE, R. V.; MARTÍNEZ, J. D. Experimental study on biomass (eucalyptus spp.) gasification in a two-stage downdraft reactor by using mixtures of air, saturated steam and oxygen as gasifying agents. **Energy Conversion and Management**, v. 145, p. 314-323, 2017.

SUSASTRIAWAN, A. A. P.; SAPTOADI, H.; PURNOMO, H.. Small-scale downdraft gasifiers for biomass gasification: a review. **Renewable And Sustainable Energy Reviews**, v. 76, p. 989-1003, 2017.

SPEIGHT, JAMES G. Unconventional gas. **Natural Gas**, p. 59-98, 2019.

SINGH, D. K.; RAJ, R.; TIRKEY, J. V.; JENA, P.; PARTHASARATHY, P.; MCKAY, G.; AL-ANSARI, T. Progress and utilization of biomass gasification for decentralized energy generation: an outlook & critical review. **Environmental Technology Reviews**, v. 12, n. 1, p. 1-36, 2023.

TEZER, Ö.; KARABAĞ, N.; ÖNGEN, A.; ÇOLPAN, C. Ö.; AYOL, A. Biomass gasification for sustainable energy production: a review. **International Journal of Hydrogen Energy**, v. 47, n. 34, p. 15419-15433, 2022.

WANG, Y.; YOSHIIE, R.; UEKI, Y.; NARUSE, I.. Characteristics of biomass gasification by oxygen-enriched air in small-scale auto-thermal packed-bed gasifier for regional distribution. **Fuel**, v. 342, p. 127852, 2023.

WANG, T.; YANG, Q.; WANG, Y.; WANG, J.; ZHANG, Y.; PAN, W-P. Arsenic release and transformation in co-combustion of biomass and coal: effect of mineral elements and volatile matter in biomass. **Bioresource Technology**, v. 297, p. 122388, 2020.

WU, R.; BEUTLER, J.; BAXTER, L. L. Biomass char gasification kinetic rates compared to data, including ash effects. **Energy**, v. 266, p. 126392, 2023.

WEI, J.; WANG, M.; WANG, F.; SONG, X.; YU, G.; LIU, Y.; VUTHALURU, H.; XU, J.; XU, Y.; ZHANG, H. A review on reactivity characteristics and synergy behavior of biomass and coal Co-gasification. **International Journal of Hydrogen Energy**, v. 46, n. 33, p. 17116-17132, 2021.

VALIN, S.; RAVEL, S.; VINCENT, P. P.; THIERY, S.; MILLER, H. Fluidized bed air gasification of solid recovered fuel and woody biomass: influence of experimental conditions on product gas and pollutant release. **Fuel**, v. 242, p. 664-672, 2019.

YANG, M.; MOUSAVI, S. M.; FATEHI, H.; BAI, X-S. Numerical simulation of biomass gasification in fluidized bed gasifiers. **Fuel**, v. 337, p. 127104, 2023.

ZHANG, Y.; CUI, Y.; CHEN, P.; LIU, S.; ZHOU, N.; DING, K.; FAN, L.; PENG, P.; MIN, M.; CHENG, Y. Gasification Technologies and Their Energy Potentials. **Sustainable Resource Recovery and Zero Waste Approaches**, p. 193-206, 2019.